

An Adaptive Observer for Sensorless Control of the Levitated Ball Using Signal Injection

Bowen Yi, Romeo Ortega, Houria Siguerdidjane and Weidong Zhang

Abstract—In this paper we address the problem of sensorless control of the 1-DOF magnetic levitation system. Assuming that only the current and the voltage are measurable, we design an adaptive state observer using the technique of signal injection. Our main contribution is to propose a new filter to identify the virtual output generated by the signal injection. It is shown that this filter, designed using the dynamic regressor extension and mixing estimator, outperforms the classical one. Two additional features of the proposed observer are that (i) it does not require the knowledge of the electrical resistance, which is also estimated on-line and (ii) exponential convergence to a tunable residual set is guaranteed without excitation assumptions. The observer is then applied, in a certainty equivalent way, to a full state-feedback control law to obtain the sensorless controller, whose performance is assessed via simulations and experiments.

I. INTRODUCTION

Magnetic levitation (MagLev) systems are widely used in industry, *e.g.*, rocket-guiding projects, high speed rail transportation, bearingless motors, vibration isolation, magnetic bearing, bearingless pumps, and microelectromechanical systems, see [8], [17] for recent reviews of Maglev systems applications. The inherent instability and high nonlinearity of MagLev systems, make them a theoretical benchmark in the nonlinear control community, with a prototype example being the simple levitated ball.

Detecting the position of the moving objects in MagLev systems needs highly expensive sensors, which usually have low accuracies. These facts stimulate the research for sensorless (also called self-sensing) control of MagLev systems, which require only the measurement of the electrical coordinates. Several technologically motivated sensorless controller have been reported by the applications community [17]. However, to the best of the authors' knowledge, besides some results based on linearized models, *e.g.*, [7], [10], there are no model-based designs reported in the control community—even for the widely studied levitated ball. One plausible explanation for this situation is that the dynamic structure of Maglev systems does not fit into the mathematically-oriented structures studied by the observer design community [2], [6],

This paper is supported by the National Natural Science Foundation of China (61473183, U1509211), China Scholarship Council, the Government of Russian Federation (074U01), the Ministry of Education and Science of Russian Federation (14.Z50.31.0031). (*Corresponding author: W. Zhang.*)

Bowen Yi and Weidong Zhang are with Department of Automation, Shanghai Jiao Tong University, Shanghai 200240, China yibowen@ymail.com, wdzhang@sjtu.edu.cn

Romeo Ortega and Houria Siguerdidjane are with L2S, CNRS-CentraleSupélec-Université Paris Saclay, Plateau du Moulon, Gif-sur-Yvette 91192, France ortega@lss.supelec.fr, houria.siguerdidjane@centralesupelec.fr

with the additional difficulty that the system is not uniformly observable.

To overcome the first difficulty, in [3] a system-tailored observer, that exploits the particular structure of the MagLev model, and the corresponding (certainty equivalence-based) sensorless controller, were proposed. The design relies on the use of parameter estimation-based observers (PEBO) [12], which combined with the dynamic regressor extension and mixing (DREM) parameter estimation technique [1], [13], allow the reconstruction of the magnetic flux. This is later used, by two suitably designed observers for the mechanical coordinates. The loss of observability problem mentioned above, hampers the application of this scheme in “underexcited” situations, hence requiring an—*a priori* unverifiable—richness assumption.

An alternative to overcome the observability obstacle in general nonlinear systems is explored in [18] where, following [4], probing high-frequency signals are injected in the control, to generate (so-called) virtual outputs used for the observer design. To detect the virtual output, the filter proposed in [4], see also [5], is applied for PEBO design to the levitated ball and a two-tank system in [18]. Although the correct asymptotic behavior of the filter is theoretically guaranteed, a bad transient performance, and strong sensitivity to the tuning—and system—parameters was observed for the levitated ball. In particular, the performance was significantly degraded with variations in the systems resistance, that are unavoidable in a practical situation.

In this paper we propose to replace the aforementioned filter by an adaptive scheme that, besides ensuring a better transient performance, removes the need of knowing the systems resistance. Similarly to [3], the design of the new filter and the resistance estimator, use the DREM estimator, yielding a gradient descent-like adaptive observer. As usual in DREM [1], [13], a key step is the suitable choice of the operators used for the construction of the extended regressor matrix. A central contribution of the paper is to propose a weighted zero-order-hold (WZOH) operator [9], which combined with a delay operator, generates a suitable scalar regressor that—due to the use of probing signals—verifies the excitation condition required to recover the virtual output. Using the latter, flux, position and velocity of the levitated ball system are, then, easily estimated. It is shown that the estimation errors converge exponentially fast into a tunable residual set, thus ensuring some good robustness properties.

The remainder of the paper is organized as follows. Section II briefly introduces the model of the levitated ball and formulates its state observer and sensorless control

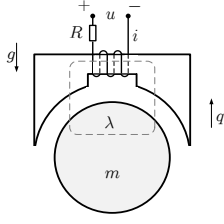


Fig. 1. Schematic diagram of the 1-DOF MagLev systems

problems. Section III presents the new robust virtual output estimator. In Sections IV and V, the adaptive observer is designed and analyzed. Simulations and experimental results are given in Section VI. The paper is wrapped-up with concluding remarks and future research directions in VII.

Notation. ϵ_t is a generic exponentially decaying term with a proper dimension. With the standard abuse of notation, the Laplace transform symbol s is used also to denote the derivative operator $\frac{d}{dt}$. \mathcal{O} is the uniform big O symbol, that is, $f(z, \epsilon) = \mathcal{O}(\epsilon)$ if and only if $|f(z, \epsilon)| \leq C\epsilon$, for a constant C independent of z and ϵ . For an operator \mathcal{H} acting on a signal we use the notation $\mathcal{H}[\cdot](t)$, when clear from the context, the argument t is omitted.

II. MODEL AND PROBLEM FORMULATION

The classical model of the unsaturated, levitated ball depicted in Fig. 1 is given as [17]

$$\begin{aligned} \dot{\lambda} &= -Ri + u \\ \dot{q} &= \frac{1}{m}p \\ \dot{p} &= \frac{1}{2k}\lambda^2 - mg \\ \lambda &= \frac{k}{c-q}i, \end{aligned} \quad (1)$$

where λ is the flux linkage, i the current, $q \in (-\infty, c)$ is the position of the ball, p is the momenta, u is the input voltage, $R > 0$ is the resistance, and $m > 0$, $c > 0$ and $k > 0$ are some constant parameters.

To simplify the notation in the sequel we introduce a change of coordinate for the position and, denoting

$$x := \text{col}(\lambda, q - c, p),$$

write the system dynamics in the standard form $\dot{x} = f(x) + gu$ with

$$f(x) := \begin{bmatrix} \frac{R}{k}x_1x_2 \\ \frac{1}{m}x_3 \\ \frac{1}{2k}x_1^2 - mg \end{bmatrix}, \quad g := \begin{bmatrix} 1 \\ 0 \\ 0 \end{bmatrix}, \quad (2)$$

and define an output

$$y = h(x) := x_1x_2, \quad (3)$$

which clearly satisfies $y = -ki$. In this paper we provide a solution to the following.

Adaptive State Observer Problem. Consider the dynamics of the levitated ball (1), represented in the form $\dot{x} = f(x) + gu$, $y = h(x)$, with (2) and (3), the parameters m , c and k known, and R unknown. Design an adaptive observer

$$\begin{aligned} \dot{\chi} &= F(\chi, u, y) \\ \hat{x} &= H(\chi, u, y) \end{aligned} \quad (4)$$

where $\chi \in \mathbb{R}^{n_\chi}$ is the observer state, such that

$$\limsup_{t \rightarrow \infty} |\hat{x}(t) - x(t)| \leq \mathcal{O}(\epsilon) \quad (5)$$

with $\epsilon > 0$ a tunable (small) constant.

As usual in observer design problems we need the following.

Assumption 1: Consider the system (1) with input (8). The controller signal u_C is such that all the states are *bounded*.¹

The sensorless controller is obtained applying certainty equivalence to the linear, static-state feedback, asymptotically stabilizing, interconnection and damping assignment passivity-based control (IDA-PBC) reported in [11], to ensure

$$\limsup_{t \rightarrow \infty} |q(t) - q_*| \leq \mathcal{O}(\epsilon), \quad (6)$$

where q_* is the desired position for the levitated ball.

Remark 1: We make the important observation that it is possible to show that the system does not satisfy the observability rank condition [Section 1.2.1][2], therefore it is not uniformly differentially observable.

III. SIGNAL INJECTION AND VIRTUAL OUTPUT FILTER

In order to overcome the lack of observability problem, we follow the signal injection method proposed in [4], and further elaborated in [18], to generate a new “virtual” output. As shown in those papers the latter is given by

$$y_v = \left(\frac{\partial h(x)}{\partial x} \right)^\top g = x_2. \quad (7)$$

To generate y_v , we add to the *controller output*, denoted u_C , a high-frequency sinusoidal signal s to generate the actual input to the system, that is,

$$\begin{aligned} u &= u_C + s \\ s(t) &= A_0 \sin\left(\frac{2\pi}{\epsilon}t\right), \end{aligned} \quad (8)$$

with $\epsilon > 0$. As shown in [4], [18], a second-order averaging analysis establishes that, there exists $\epsilon_* > 0$ such that, for all $\epsilon \in (0, \epsilon_*]$, we have that the following identity in the interval $[t, t + \mathcal{O}(1/\epsilon))$,

$$\begin{aligned} x_1 &= \bar{x}_1 + \epsilon S + \mathcal{O}(\epsilon^2) \\ x_2 &= \bar{x}_2 + \mathcal{O}(\epsilon^2) \\ x_3 &= \bar{x}_3 + \mathcal{O}(\epsilon^2), \end{aligned} \quad (9)$$

¹To avoid cluttering the notation we use the generic symbol κ to denote a positive constant that upperbounds all signals.

where S is the primitive of s , that is,

$$S(t) := -\frac{A_0}{2\pi} \cos\left(\frac{2\pi}{\varepsilon}t\right), \quad (10)$$

and the overline denotes the states of the average system, namely,

$$\dot{\bar{x}} = f(\bar{x}) + gu_C \quad (11)$$

with $\bar{x}(0) = x(0)$. Some simple calculations show that

$$y = \bar{y} + \varepsilon S y_v + \mathcal{O}(\varepsilon^2), \quad (12)$$

with $\bar{y} := \bar{x}_1 \bar{x}_2$.

To simplify the notation, and with some obvious abuse of notation, in the sequel we omit the clarification that the averaging analysis only insures the existence of a lower bound on ε such that (9) holds, and we simply assume that ε is small enough.

We recall that the problem is to reconstruct y_v out of the measurement of y , for which a sliding-window filter is proposed in [4], and also used in [18]. As discussed in the introduction, the use of this filter generated some serious robustness problem. Consequently, we propose in this paper to replace it by an estimator that, similarly to DREM, implements a gradient descent observer based on a suitable linear regression model.

The first step is then to obtain the linear regression model, making the key observation that, with respect to S , the signals \bar{y} and y_v are slowly time-varying. This motivates us to view (12) as a linear (time-varying) regression perturbed by a small term $\mathcal{O}(\varepsilon^2)$. Whence, we write (12) as

$$\begin{aligned} y &= \phi^\top \theta + \mathcal{O}(\varepsilon^2) \\ \theta &:= \text{col}(\bar{y}, \varepsilon y_v) \\ \phi &:= \text{col}(1, S), \end{aligned} \quad (13)$$

with y the measurable signal, and ϕ and θ playing the roles of known regressor and (slowly time-varying) parameters to be estimated.

We will estimate the parameters θ using the DREM estimator—we refer the reader to [1] for additional details on DREM. The main idea of DREM is to generate from (13) a *scalar* regression for the “parameter” of interest, in this case, $\theta_2 = \varepsilon y_v$. Although this can be achieved with arbitrary \mathcal{L}_∞ -stable, linear operators, the resulting scalar regressor does not necessarily satisfy the excitation conditions required to ensure parameter convergence. It turns out that in our case, the latter is possible, selecting some specific operators as detailed in the lemma below, whose proof is given in the Appendix.

To streamline the presentation of the lemma we define two \mathcal{L}_∞ -stable, linear operators, first, the delay operator \mathcal{H}_d , with parameter $d > 0$,

$$\mathcal{H}_d[v](t) = v(t-d). \quad (14)$$

Second, the WZOH operator [9] \mathcal{Z}_w , parameterized by $w > 0$, defined as

$$\begin{aligned} \dot{\chi}(t) &= v(t) \\ \mathcal{Z}_w[v](t) &= \frac{1}{w} [\chi(t) - \chi(t-w)]. \end{aligned} \quad (15)$$

Lemma 1: Consider the linear regression (13) and the operators \mathcal{H}_d (14) and \mathcal{Z}_w (15), with $w = 2d$ and $d = n\varepsilon$, for some $n \in \mathbb{Z}_+$. Then,

$$Y(t) = S(t-d)\theta_2(t-d) + \mathcal{O}(\varepsilon^2), \quad (16)$$

where we defined the measurable signal

$$Y := (\mathcal{H}_d - \mathcal{Z}_{2d})[y]. \quad (17)$$

In the proposition below, we propose a simple gradient descent algorithm to identify θ_2 from (16).

Proposition 1: Consider the system (1) with measurable output (3) and input (8) verifying Assumption 1. Define the virtual output estimator

$$\begin{aligned} \dot{\hat{\theta}}_2 &= \gamma S(t-d)[Y(t) - S(t-d)\hat{\theta}_2] \\ \hat{y}_v &= \frac{\hat{\theta}_2}{\varepsilon}, \end{aligned} \quad (18)$$

where $\gamma > 0$ is a tuning gain, S is given in (10), Y in (17), \mathcal{H}_d and \mathcal{Z}_{2d} are defined in (14) and (15), respectively, with $d = n\varepsilon$, for some $n \in \mathbb{Z}_+$. Then,

$$\lim_{t \rightarrow \infty} |\hat{y}_v(t) - y_v(t)| \leq \mathcal{O}(\varepsilon) \quad (\text{exp.}), \quad (19)$$

where y_v is defined in (7).

Proof: Define the error signal

$$\tilde{\theta}_2 := \hat{\theta}_2 - \varepsilon y_v.$$

Invoking Lemma 1, and replacing (16) in (18) we get

$$\dot{\tilde{\theta}}_2 := -\gamma S^2(t-d)\tilde{\theta}_2 + \mathcal{O}(\varepsilon). \quad (20)$$

From (10) it is clear that $S(t)$ satisfies

$$\int_t^{t+\varepsilon} S^2(\mu-d)d\mu \geq S_0$$

for any t and some $S_0 > 0$. Therefore, some basic perturbation analysis completes the proof. ■

Remark 2: The virtual output filters in [4], [18] compute the estimate of the virtual output by averaging in a moving horizon $[t-n\varepsilon, t]$ the observation error—that is, in fact, an open-loop design. The new filter (18) provides an alternative *closed-loop* approach, making it robust to unavoidable measurement noise.

IV. ADAPTIVE OBSERVER DESIGN

In this section we design the adaptive state observer using the estimate of y_v of Proposition 1. To enhance readability it is split into three subsections presenting, respectively, the resistance estimator, the flux observer and the observer for position and velocity.

A. Resistance identification

Before presenting the resistance estimator we make the observation that, due to the physical constraints $q \in (-\infty, c)$. As expected, we impose this constraint also to its estimate,² hence

$$\begin{aligned} y_v &= q - c \leq \ell < 0 \\ \hat{y}_v &\leq \ell < 0. \end{aligned} \quad (21)$$

As expected in adaptive systems design it is necessary to impose an excitation constraint.

Assumption 2: Consider the system (1) with input (8). The current i is persistently exciting (PE), that is, there exist $T_i > 0$ and $\delta_i > 0$ such that

$$\int_t^{t+T_i} i^2(\tau) d\tau \geq \delta_i, \quad (22)$$

for all $t \geq 0$.

Proposition 2: Consider the system (1) with input (8) verifying Assumptions 1 and 2. Define the resistance estimator as

$$\dot{\hat{R}} = \gamma_R \phi_R (Y_R - \phi_R \hat{R}) \quad (23)$$

with $\gamma_R > 0$ a tuning gain, and

$$\begin{aligned} \dot{v}_1 &= -av_1 + au \\ \dot{v}_2 &= -av_2 + a \left(\frac{y}{\hat{y}_v} \right) \\ \dot{\phi}_R &= -a\phi_R + \frac{a}{k} y \\ Y_R &= -v_1 + a \frac{y}{\hat{y}_v} - av_2, \end{aligned} \quad (24)$$

with $a > 0$ and \hat{y}_v generated as in Proposition 1. Then,

$$\lim_{t \rightarrow \infty} |\hat{R}(t) - R| \leq \mathcal{O}(\varepsilon) \quad (\text{exp.})$$

Proof: From (3) and (7) we have the relationship $x_1 = \frac{y}{\hat{y}_v}$, which is well defined in view of (21). Computing the derivative with respect to time yields

$$\frac{d}{dt} \left(\frac{y}{\hat{y}_v} \right) = R \frac{y}{k} + u.$$

Applying to the equation above the linear time invariant (LTI) filter $\frac{a}{s+a}$ yields

$$\frac{as}{s+a} \left[\frac{y}{\hat{y}_v} \right] - \frac{a}{s+a} [u] = R \frac{a}{s+a} [y] + \epsilon_t, \quad (25)$$

where ϵ_t is an exponentially decaying term stemming from the filters initial conditions. As shown in [1], without loss of generality, this term is neglected in the sequel.

Notice now that (24) is a state realization of the filters

$$\begin{aligned} Y_R &= \frac{as}{s+a} \left[\frac{y}{\hat{y}_v} \right] - \frac{a}{s+a} [u] \\ \phi_R &= \frac{a}{s+a} [y], \end{aligned} \quad (26)$$

²This can easily be done adding a projection operator to the second equation in (18), but is omitted for brevity.

Motivated by this fact define the auxiliary (ideal) dynamics

$$\dot{v}_2^* = -av_2^* + a \left(\frac{y}{\hat{y}_v} \right).$$

and the signal

$$Y_R^* := -v_1 + a \frac{y}{\hat{y}_v} - av_2^*,$$

and notice that (25) may be written as

$$Y_R^* = R \phi_R.$$

Define the signal $\tilde{Y}_R := Y_R - Y_R^*$, which upon replacement in (23), yields

$$\dot{\tilde{R}} = -\gamma_R \phi_R^2 \tilde{R} + \gamma_R \phi_R \tilde{Y}_R, \quad (27)$$

where we defined the resistance estimation error $\tilde{R} := \hat{R} - R$. Exponential convergence to zero of the unperturbed dynamics follows invoking the PE Assumption 2 and standard adaptive control arguments [14].

To analyse the stability of (27) define the error $\tilde{v}_2 := v_2 - v_2^*$, whose dynamics is given as

$$\dot{\tilde{v}}_2 = -a\tilde{v}_2 + ay \left(\frac{1}{\hat{y}_v} - \frac{1}{y_v} \right). \quad (28)$$

Now, we recall (21), from which we get the following inequality

$$\left| \frac{1}{y_v} - \frac{1}{\hat{y}_v} \right| = \left| \frac{\tilde{y}_v}{y_v \hat{y}_v} \right| \leq \frac{1}{\ell^2} |\tilde{y}_v|,$$

where we defined $\tilde{y}_v := \hat{y}_v - y_v$. Using (19) and the inequality above, and invoking Assumption 1 that ensures $|y| \leq \kappa$, from (28) we conclude that

$$\lim_{t \rightarrow \infty} |\tilde{v}_2(t)| \leq \mathcal{O}(\varepsilon). \quad (29)$$

The proof is completed noting that a similar property holds for \tilde{Y}_R and invoking the exponential stability of the unperturbed dynamics. ■

Remark 3: The assumption that i is PE is not restrictive at all. Actually it is possible to show that this condition can be transferred to the control u .³ Now, since u defined in (8) contains an additive term that is PE, the condition that u is PE will almost always be satisfied.

B. Flux observer

Before presenting our observer notice that the flux x_1 admits the following algebraic observer

$$\hat{x}_1 = \frac{y}{\hat{y}_v}. \quad (30)$$

Unfortunately, due to the division operation, such a design is relatively sensitive to measurement noise, making it non-robust.⁴ To overcome this drawback, we propose below a closed-loop flux observer design.

³The details of this proof are omitted for brevity.

⁴In the resistance estimator, although such relationship is used, the LTI filter and the closed-loop gradient descent dynamics reduce the deleterious effects significantly.

Proposition 3: Consider the system (1) with measurable output (3) and input (8) verifying Assumptions 1 and 2. Define the flux observer

$$\dot{\hat{x}}_1 = \frac{\tilde{R}}{k}y + u - \gamma_\lambda(y - \hat{y}_v\hat{x}_1). \quad (31)$$

with $\gamma_\lambda > 0$ and \hat{y}_v, \hat{x}_1 generated as in Propositions 1 and 3, respectively. Assume the current i verifies (22). Then,

$$\lim_{t \rightarrow \infty} |\hat{x}_1(t) - x_1(t)| \leq \mathcal{O}(\varepsilon) \quad (\text{exp.})$$

Proof: From (31) we get

$$\begin{aligned} \dot{\hat{x}}_1 &= \frac{R}{k}y + u - \gamma_\lambda(y - \hat{y}_v\hat{x}_1) + \frac{\tilde{R}}{k}y \\ &= \dot{x}_1 - \gamma_\lambda(y - y_v\hat{x}_1) + \frac{\tilde{R}}{k}y + \gamma_\lambda\tilde{y}_v\hat{x}_1. \end{aligned}$$

Define the flux estimation error $\tilde{x}_1 := \hat{x}_1 - x_1$, whose dynamics is given as

$$\dot{\tilde{x}}_1 = \gamma_\lambda y_v \tilde{x}_1 + \frac{\tilde{R}}{k}y + \gamma_\lambda \tilde{y}_v \hat{x}_1.$$

From (21) we see that the unperturbed dynamics is exponentially stable and, moreover, from (31) we have that \hat{x}_1 is bounded. The proof is completed using these two properties and invoking Propositions 1 and 2. ■

C. Position and momenta observer

Given the definition of the virtual output (7), we trivially obtain an algebraic observer for x_2 as follows

$$\hat{x}_2 = \hat{y}_v. \quad (32)$$

To obtain an observer for the momenta x_3 we follow the Kazantzis-Kravaris-Luenberger (KKL) methodology [13] in the proposition below.

Proposition 4: Consider the system (1) with measurable output (3) and input (8) verifying Assumptions 1 and 2. Define the momenta observer

$$\begin{aligned} \dot{z} &= -\frac{\gamma_p}{m}z + \frac{1}{2k}\hat{x}_1^2 - \frac{\gamma_p^2}{m}\hat{y}_v - mg \\ \hat{x}_3 &= z + \gamma_p\hat{y}_v, \end{aligned} \quad (33)$$

with $\gamma_p > 0$ and \hat{y}_v, \hat{x}_1 generated as in Propositions 1 and 3, respectively. Then,

$$\lim_{t \rightarrow \infty} |\hat{x}_3(t) - x_3(t)| \leq \mathcal{O}(\varepsilon) \quad (\text{exp.})$$

Proof: Define the signal

$$T := x_3 - \gamma_p y_v. \quad (34)$$

Notice that, from the second equation of (33) and (34), we get

$$\hat{x}_3 - x_3 = z - T + \gamma_p \tilde{y}_v. \quad (35)$$

As usual in KKL observers, the gist of the proof is to show that z ‘‘approaches’’ T . Now, differentiating (34) we have

$$\dot{T} = -\frac{\gamma_p}{m}T - \frac{\gamma_p^2}{m}y_v + \frac{1}{2k}x_1^2 - mg.$$

Using the first equation of (33) we get

$$\dot{T} - \dot{z} = -\frac{\gamma_p}{m}(T - z) + -\frac{\gamma_p^2}{m}\tilde{y}_v - \frac{1}{2k}(\hat{x}_1\tilde{x}_1 - \tilde{x}_1^2)$$

From the equation above we conclude that

$$\lim_{t \rightarrow \infty} |z(t) - T(t)| \leq \mathcal{O}(\varepsilon) \quad (\text{exp.})$$

The proof is completed replacing (19) and the limit above in (35). ■

Remark 4: An alternative to the KKL observer above is a standard Luenberger observer

$$\begin{aligned} \dot{z}_1 &= \frac{1}{m}z_2 + c_1(\hat{x}_2 - z_1) \\ \dot{z}_2 &= \frac{1}{2k}\hat{x}_1^2 - mg + c_2(\hat{x}_2 - z_2) \\ \hat{x}_3 &= z_2, \end{aligned}$$

with $c_1 > 0$ and $c_2 > 0$. However, the order of such a design is higher than that of the KKL observer (33). Moreover, as shown in Section VI-A it was observed in simulations that the KKL observer outperforms the Luenberger one and is easier to tune.

V. ADAPTIVE OBSERVER AND SENSORLESS CONTROLLER

To solve the adaptive state observation of Section II we summarize in this section the derivations presented in the previous section. Also, we propose a sensorless controller.

Proposition 5: Consider the system $\dot{x} = f(x) + gu$, $y = h(x)$, with (2) and (3), with input (8) verifying Assumptions 1 and 2. The 7-order adaptive observer (4) with mappings

$$F = \begin{bmatrix} -\gamma S(t-d)[Y(t) - S(t-d)\chi_1] \\ -a\chi_2 + au \\ -a\chi_3 + a\left(\frac{y}{\varepsilon\chi_1}\right) \\ -a\chi_4 + \frac{a}{k}y \\ \gamma_R\chi_4\left(\chi_2 + a\frac{y}{\varepsilon\chi_1} - a\chi_3 - \chi_4\chi_5\right) \\ -\frac{1}{k}y\chi_5 + u - \gamma_\lambda(y - \varepsilon\chi_1\chi_6) \\ \frac{\gamma_p}{m}\chi_7 + \frac{2}{2k}\chi_6^2 - \frac{\gamma_p^2}{m}\varepsilon\chi_1 - mg \end{bmatrix}$$

$$H = \begin{bmatrix} \chi_6 \\ \varepsilon\chi_1 \\ \chi_7 + \gamma_p\varepsilon\chi_1 \end{bmatrix},$$

with Y given in (17) and $a, \gamma, \gamma_R, \gamma_\lambda, \gamma_p > 0$, guarantees (5).

Proof: The proof is established identifying

$$\chi = \text{col}(\hat{\theta}_2, v_1, v_2, \phi_R, \hat{R}, \hat{x}_1, z),$$

and invoking the results of Propositions 1-4. ■

We are in position to give the sensorless control law, which is a certainty equivalence version of the IDA-PBC given in [11]. Namely

$$u_C = -\frac{1}{k}\chi_5 y - K_p \left(\frac{1}{\alpha}(\chi_6 - \lambda_*) + (\varepsilon\chi_1 + c - q_*) \right) - \left(\frac{\alpha}{m} + K_p \right) (\chi_7 + \gamma_p \varepsilon \chi_1) \quad (36)$$

where λ_* and q_* are the desired values for λ and q , respectively, and $K_p, \alpha > 0$ are some tuning constants.

VI. SIMULATIONS AND EXPERIMENTS

In this section, the performance of the novel observer is validated via computer simulations and experiments. All simulations are conducted by Matlab/Simulink. The parameters used in the simulation and the control of the experimental rig are in Table I. The new design is compared, via simulations, with the one in [18]. In both simulations and experiments, the desired equilibrium is $(\sqrt{2kmg}, q_*, 0)$, with q_* taken as a pulse train, and with the initial states $(\sqrt{2kmg}, 0, 0)$.

TABLE I

PARAMETERS OF MAGLEV SYSTEMS: SIMULATION (FIRST COLUMN) AND EXPERIMENTS (SECOND COLUMN)

Ball mass [kg]	0.0844	0.0844
Gravitational acceleration [m/s ²]	9.81	9.81
Resistance [Ω]	2.52	10.615
Position [m]	0.005	0.0079
Inductance constant (k) [$\mu\text{H}\cdot\text{m}$]	6404.2	49950

A. Performance of the observer

For a fair comparison with the observer design in [18], simulations are run with the state-feedback version of the controller (36), whose parameters are set as $K_p = 200.7, \alpha = 33.4$. To make simulations more realistic, we add measurement noise in the current i , which is generated with the ‘‘Uniform Random Number’’ block in Matlab/Simulink, within $[-0.003, 0.003]\text{A}$.

The parameters in the proposed observer are selected as $A_0 = 1, \varepsilon = 1/300, d = 10\varepsilon, a = 500, \gamma = 3.89 \times 10^3, \gamma_R = 500, \gamma_\lambda = 8000, \gamma_p = 30$. The parameters of the design in [18] are selected as $n = 5, \varepsilon = 1/300, \alpha = 0.01, \gamma = 50$.

Simulation results in Matlab/Simulink are shown in Figs. 2-3, where $(\hat{\cdot})^*$ denotes the results from the filter in [18]. To compare the two momenta observers proposed in Subsection VI-C, we have included that estimate \hat{p}_L , computed by the Luenberger observer (33). As expected, the new design is less sensitive to measurement noise due to its closed-loop structure, and also, the steady-state observation are of the accuracy $\mathcal{O}(\varepsilon)$. Besides, the KKL observer outperforms the Luenberger one.

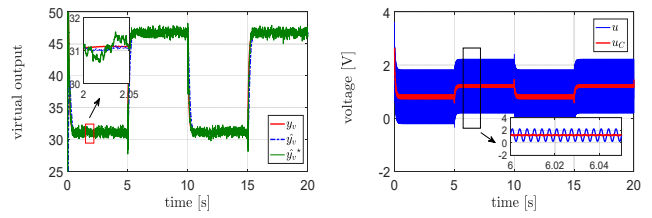


Fig. 2. Virtual output estimation and input (simulation)

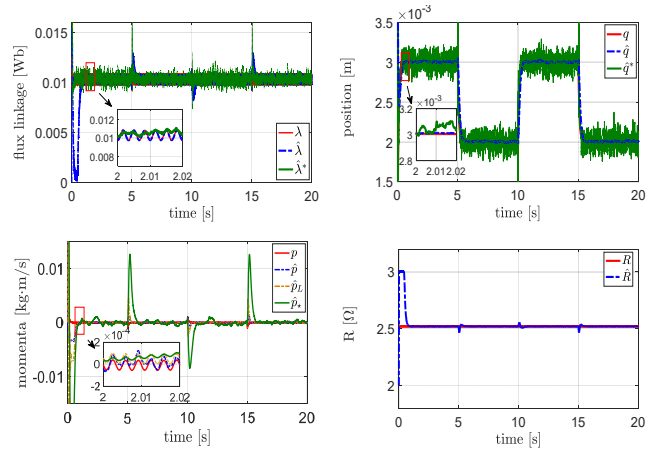


Fig. 3. State and parameter estimations (simulation)

B. Performance of the sensorless controller

In this section, we test the current feedback IDA-PBC law (36) with the same parameters as those in Subsection VI-A. We observe in Fig. 4 that the position has a significant regulation error in the first second, which is due to the initial inaccurate estimation of R . However, the remaining transients are very satisfactory and almost identical to the state-feedback IDA-PBC.

C. Experiments

Some experiments have been conducted on the experimental set-up of the 1-DOF MagLev system shown in Fig. 5, which is located at the laboratory at D epartement Automatique, CentraleSup elec. The proposed adaptive observer was tested in closed-loop with the following well-tuned

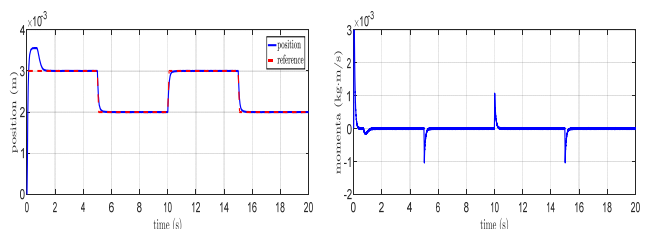


Fig. 4. States with sensorless control (36)

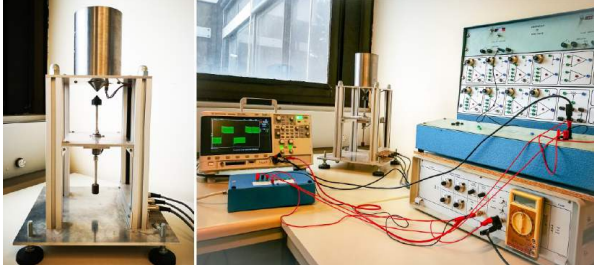


Fig. 5. Experimental set-up

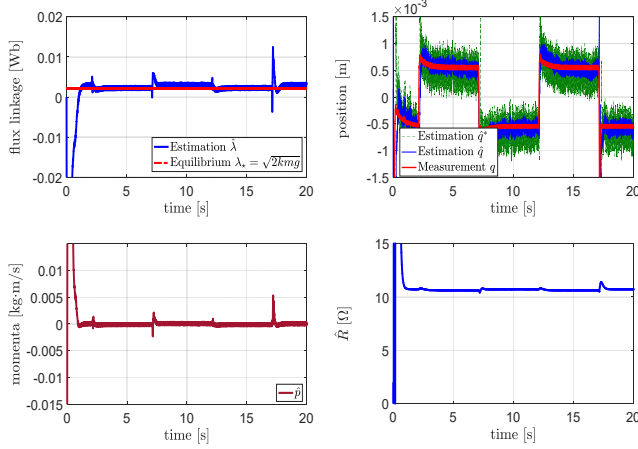


Fig. 6. State and parameter estimations (experiment)

backstepping+integral controller

$$u_0 = R(c - q)\sqrt{|\Upsilon|}\text{sign}(\Upsilon) - K_i \int_0^t (q - q_*) d\tau$$

$$\Upsilon(q, p) = \frac{2}{k}(mg - \gamma_1(p - p_*) - \gamma_2 m(q - q_*)),$$

with $K_i = 1$, $\gamma_1 = 340$ and $\gamma_2 = 3$. The parameters in the observer are taken as $A_0 = 1.5$, $\varepsilon = 0.03$, $d = 10\varepsilon$, $a = 10$ and $\gamma = 360$, $\gamma_R = 50$, $\gamma_\lambda = 8 \times 10^3$, $\gamma_p = 20$.

The responses are shown in Figs. 6-7, where we also give the position estimate \hat{q}^* from the design in [18]. Unfortunately, the device is only equipped with sensors for position and current. Hence, we can only compare the position estimate with its measured values, as well as the flux linkage estimate with its desired equilibrium. Again, we verify the accuracy and the robustness of the new observer in the presence of measurement noise. Fig. 8 gives the position estimates with different probing frequencies. It illustrates that a higher frequency yields a higher accuracy, but at the price of a more jittery response.

VII. CONCLUDING REMARKS

In this work we present a novel method for adaptive state observation of a 1-DOF MagLev system, measuring only the coil current and without the knowledge of the electrical resistance. A gradient-descent (like) observer based on DREM is proposed and proven to guarantee—without imposing an excitation assumption—exponential convergence to an (arbitrarily small) residual set. The performance of the

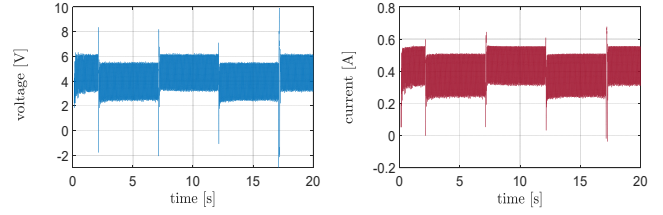


Fig. 7. Input and output (experiment)

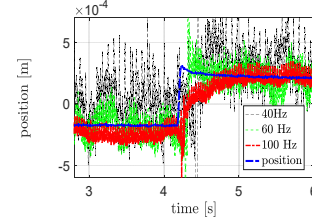


Fig. 8. Position estimation for different excitation frequencies

observer, and its application in a sensorless controller, has been verified by simulations and experiments.

Some remarks are in order.

- The 1-DOF MagLev system is a benchmark of electromechanical systems. We are currently investigating the application of the new observer to other electromechanical systems—in particular, electrical motors [19].
- Signal injection is a widely-used technique-oriented method for electromechanical systems. With the notable exception of [4], [5], no theoretical analysis can be found in the literature. It is challenging to establish the connection between the proposed method and the standard techniques in industry, or provide a theoretical interpretation to the existing technique-oriented methods [20].
- Although we analyze the effects of the probing frequencies from the theoretical viewpoint, there are many practical considerations that must be taken into account before claiming it to be an operational technique.
- The simulations and experiments were conducted in the Matlab/Simulink with continuous modules, and as observed the computational efficiency is relatively low. It is of practical interests to give a computationally high-efficient digital implementation of the proposed method.

REFERENCES

- [1] S. Aranovskiy, A. Bobtsov, R. Ortega and A. Pyrkin, Performance enhancement of parameter estimators via dynamic regressor extension and mixing, *IEEE Trans. Automatic Control*, vol. 62, pp. 3546-3550, 2017.
- [2] G. Besançon (ed.), *Nonlinear Observers and Applications*, Springer, Berlin, Lecture Notes in Control and Information Sciences, 2007.
- [3] A. Bobtsov, A. Prykin, R. Ortega and A. Vedyakov, State observers for sensorless control of magnetic levitation systems, *Automatica*, to be published. (arXiv:1711.02733)
- [4] P. Combes, A.K. Jebai, F. Malrait, P. Martin and P. Rouchon, Adding virtual measurements by signal injection, *American Control Conference (ACC)*, Boston, USA, July 6-8, 2016, pp. 999-1005, 2016.

- [5] P. Combes, F. Malrait, P. Martin and P. Rouchon, An analysis of the benefits of signal injection for low-speed sensorless control of induction motors, *International Symposium on Power Electronics, Electrical Drives, Automation and Motion*, Anacapri, Italy, June 22-24, pp. 721-727, 2016.
- [6] J.P. Gauthier and I. Kupka, *Deterministic Observation Theory and Applications*, Cambridge University Press, 2001.
- [7] T. Glück, W. Kemmettmüller, C. Tump, A. Kugi, A novel robust position estimator for self-sensing magnetic levitation systems based on least squares identification, *Control Engineering Practice*, vol 19, pp. 146-157, 2011.
- [8] H. Han and D. Kim, *Magnetic Levitation: Maglev Technology and Applications*, Springer-verlag, London, 2016.
- [9] R. Middleton and G. Goodwin, *Digital Control and Estimation: A Unified Approach*, Prentice Hall, NJ, 1990.
- [10] T. Mizuno, K. Araki and H. Bleuler, Stability analysis of self-sensing magnetic bearing controllers, *IEEE Trans. Control Systems Technology*, vol. 4, pp. 572-579, 1996.
- [11] R. Ortega, A.J. van der Schaft, I. Mareels and B. Maschke, Putting energy back in control, *IEEE Control Systems Magazine*, vol. 21, pp. 18-33, 2001.
- [12] R. Ortega, A. Bobtsov, A. Pyrkin, S. Aranovskiy, A parameter estimation approach to state observation of nonlinear systems, *Systems & Control Letters*, vol. 85, pp. 84-94, 2015.
- [13] R. Ortega, L. Praly, S. Aranovskiy, B. Yi and W. Zhang, On dynamic regressor extension and mixing parameter estimators: Two Luenberger observers interpretations, *Automatica*, vol. 95, pp. 548-551, 2018.
- [14] S. Sastry and M. Bodson, *Adaptive Control: Stability, Convergence and Robustness*, Prentice Hall, Englewood Cliffs, NJ, 1989.
- [15] A. Ranjbar, R. Noboa, B. Fahimi, Estimation of airgap length in magnetically levitated systems, *IEEE Trans. on Industry Applications*, vol. 48, pp. 2173-2181, 2012.
- [16] H. Rodriguez, H. Siguerdidjane and R. Ortega, Experimental comparison of linear and nonlinear controllers for a magnetic suspension, *Proceeding of the IEEE International Conference on Control Applications*, Anchorage, Alaska, USA, 2000.
- [17] G. Schweitzer and E. Maslen (eds.), *Magnetic Bearings: Theory, Design and Application to Rotating Machinery*, Springer-Verlag, Heidelberg, 2009.
- [18] B. Yi, R. Ortega and W. Zhang, Relaxing the conditions for parameter estimation-based observers of nonlinear systems via signal injection, *Systems & Control Letters*, vol. 111, pp. 18-26, 2018.
- [19] B. Yi, R. Ortega, H. Siguerdidjane, J.E. Machado and W. Zhang, On generation of virtual outputs via signal injection: Applications to observer design for electromechanical systems, *LSS-Supelec, Int. Report*, June, 2018.
- [20] B. Yi, S.N. Vukosavic, R. Ortega, A.M. Stankovic and W. Zhang, A new signal injection-based method for estimation of position in salient permanent magnet synchronous motors, *LSS-Supelec, Int. Report*, Apr., 2018.
- [21] B. Yi, R. Ortega and W. Zhang, On state observers for nonlinear systems: A new design and a unifying framework, *IEEE Trans. Automatic Control*, (to appear), 2018. (arXiv:1712.08209)

APPENDIX

PROOF OF LEMMA 1

First, we will prove that for any smooth signal of the form

$$r(t) = \bar{r}(t) + \varepsilon S(t)r_v(t),$$

by fixing $w = 2n\varepsilon$ in the WZOH operator with $n \in \mathbb{Z}_+$, we have

$$\mathcal{Z}_w[r](t) = \bar{r}(t - \frac{w}{2}) + \mathcal{O}(\varepsilon^2). \quad (37)$$

According to the definition of the WZOH filter, we have

$$\mathcal{Z}_w[r](t) = \frac{1}{w} \int_0^w r(t - \mu) d\mu,$$

where in the second equality we used the new variable $\mu := t - \tau$. Thus,

$$\begin{aligned} \mathcal{Z}_w[r](t) &= \frac{1}{w} \int_0^w (\bar{r}(t - \mu) + \varepsilon S(t - \mu)r_v(t - \mu)) d\mu \\ &= \frac{1}{w} \int_0^w (\bar{r}(t) - \dot{\bar{r}}(t)\mu + \frac{1}{2}\ddot{\bar{r}}(t)\mu^2 + \delta_2(t, \mu)\mu^3) d\mu \\ &\quad + \frac{\varepsilon}{w} \int_0^w (r_v(t) - \dot{r}_v(t)\mu + \delta_3(t, \mu)\mu^2) S(t) d\mu \\ &= \bar{r}(t - \frac{w}{2}) + \varepsilon w \dot{r}_v(t) \mathbb{S}(t) + \Delta_1(t, w) + \Delta_2(t, w), \end{aligned}$$

where we have used Taylor expansion—which holds for some mappings δ_2 and δ_3 —for the second and third identities, and defined \mathbb{S} , as the primitive of S , in the fourth identity, and

$$\begin{aligned} \Delta_1(t, w) &:= \frac{1}{w} \int_0^w (\frac{1}{2}\ddot{\bar{r}}(t)\mu^2 + \delta_2(t, \mu)\mu^3) d\mu \\ \Delta_2(t, w) &:= \frac{\varepsilon}{w} \int_0^w (r_v(t) + \delta_3(t, \mu)\mu^2) S(t) d\mu. \end{aligned}$$

Invoking $w = 2n\varepsilon$, it yields

$$\varepsilon w \dot{r}_v(t) \mathbb{S}(t) + \Delta_1(t, w) + \Delta_2(t, w) = \mathcal{O}(\varepsilon^2),$$

which completes the proof of the claim (37).

Now, it is obvious that,

$$\mathcal{H}_d[y](t) = [1 \quad S(t-d)] \theta(t-d). \quad (38)$$

Applying the property (37) of the WZOH filter to the signal y we get

$$\mathcal{Z}_w[y](t) = [1 \quad 0] \theta(t - \frac{w}{2}) + \mathcal{O}(\varepsilon^2). \quad (39)$$

Therefore, selecting $w = 2d$, and piling up the two new regressors (38) and (39), we get

$$\begin{bmatrix} \mathcal{H}_d[y](t) \\ \mathcal{Z}_{2d}[y](t) \end{bmatrix} = \Phi(t)\theta(t-d) + \mathcal{O}(\varepsilon^2), \quad (40)$$

where we defined the extended regressor matrix

$$\Phi(t) := \begin{bmatrix} 1 & S(t-d) \\ 1 & 0 \end{bmatrix}. \quad (41)$$

From (40) we clearly get

$$\mathcal{H}_d[y](t) - \mathcal{Z}_{2d}[y](t) = S(t-d)\theta_2(t-d) + \mathcal{O}(\varepsilon^2), \quad (42)$$

completing the proof of the Lemma.